Photocatalytic removal of pentachlorophenol by means of an enzyme-like molecular imprinted photocatalyst and inhibition of the generation of highly toxic intermediates†

Xiantao Shen,[a] Lihua Zhu,*[a] Guoxia Liu,[a] Heqing Tang,*[a] Shushen Liu[b] and Weiying Li[b]

Received (in Gainesville, FL, USA) 11th June 2009, Accepted 4th August 2009
First published as an Advance Article on the web 2nd September 2009
DOI: 10.1039/b9nj00255c

Pentachlorophenol (PCP) is a typical highly-toxic pollutant, and its direct photolysis and conventional photocatalysis may produce more toxic by-products such as dibenzodioxins. It is urgently needed to develop a photocatalytic process able to remove PCP without the generation of highly toxic by-products. To achieve this, enzyme-like molecular-imprinted photocatalysts were prepared by using structural analogues of PCP as pseudo templates. It was found that 2,4-dinitrophenol (DNP) was the best template among the tested analogues. The molecular imprinted polymer (MIP) coated P25 TiO_2 photocatalyst DNP–P25 prepared with DNP as the template greatly accelerated the photocatalytic degradation of PCP and depressed the generation of toxic intermediates. It was confirmed that the amino groups at the footprint cavities provided a well-defined micro reaction environment, which made the benzene ring of the adsorbed PCP be better exposed to photo-generated reactive OH radicals, leading to easier cleavage of the benzene ring. Both the intermediate analysis and toxicity evaluation confirmed that the MIP-coated TiO_2 can make the photocatalytic degradation a safe and green approach of removing PCP.

1. Introduction

Enzyme mimics or artificial enzymes have been synthesized as catalysts *via* molecular imprinting techniques.[1–8] The earliest work in this area dates back to the preparation of molecularly imprinted polymers (MIPs) for catalytic hydrolysis of the *p*-nitrophenyl ester of an amino acid.[1] Later, the catalytic MIPs were introduced into elimination reactions,[2] Michael addition reductions,[3] hydride transfer reductions,[4] oxidation reactions[5] and conformational reactions.[6,7] The methods to obtain MIPs with catalytic activity can also use analogues of the substrate, transition state, or products as templates.[8] There are two prerequisites for the preparation of MIPs showing enzyme-like catalytic activity. Firstly, a cavity has to be made with a defined shape corresponding to the shape of the target substrate or its transition state in the reaction. Secondly, functional groups in a defined stereochemistry must be introduced as binding sites, coenzyme analogues, or catalytic sites within the cavity.[9]

The applications of MIPs as catalysts suggests that the main reaction can be accelerated and the generation of unfavorable by-products will be inhibited.[10] This is helpful for environmental protection, because it is known that the chemical treatment of various organic pollutants is rather slow with the generation of more harmful by-products.[11] Therefore, it is possible to use an MIP catalyst for decomposing persistent organic pollutants in waste waters without producing more harmful by-products.

Recently, we have introduced MIPs into the selective photocatalytic degradation of organic pollutants.[12–15] Using *o*-phenylenediamine (OPDA) as a monomer and the target pollutants (2-chlorophenol, 4-chlorophenol, 2-nitrophenol or 4-nitrophenol) as templates, we have prepared a series of MIP-coated TiO_2 photocatalysts. These catalysts markedly promote the photocatalytic degradation of the target organic compounds, in comparison with the naked TiO_2 catalyst.[12,13] It has been found that these photocatalysts also decrease the accumulation of degradation intermediates, indicating that the photocatalytic degradation of the intermediates is accelerated at the same time.

As a more harmful phenolic pollutant, pentachlorophenol (PCP) is present in the environment mainly due to its widespread applications in agriculture and industry as an important component part of bactericides, insecticides, fungicides and wood preservatives.[16] As PCP can cause severe damage to human health even at low concentrations, it is widely recognized as one of the most toxic pollutants and listed as a priority pollutant published by the European Union in the last directive about water policy (Directive, 2000/60/EC). Several methods have been investigated for the removal of PCP from the environment. One is the biodegradation under aerobic and anaerobic conditions,[17,18] but it is slow and incomplete because of the toxicity of PCP to the organisms.[19] Direct photolysis of PCP is also slow.[20–22] Advanced oxidation processes (AOPs) such as radiolysis,[23] and the ozone,[24]

[a] *College of Chemistry and Chemical Engineering, Huazhong University of Science and Technology, Wuhan 430074, P.R. China. E-mail: lhzhu63@yahoo.com.cn, hqtang62@yahoo.com.cn; Fax: +86-27-87543632; Tel: +86-27-87543432*
[b] *Key Laboratory of Yangtze River Water Environment, Ministry of Education, College of Environmental Science and Engineering, Tongji University, Shanghai 200092, P.R. China*
† Electronic supplementary information (ESI) available: Supplementary figures showing spectra of results. See DOI: 10.1039/b9nj00255c

ozone/ultrasound,[25] Fenton,[26] and photocatalytic processes[27,28] have been investigated for treating PCP. However, the degradation in these processes is inefficient due to the accumulation of intermediates.[29] Unfortunately, more toxic intermediates are generated in the reported processes of removing PCP. For example, more harmful polychlorinated dibenzo-*p*-dioxins (PCDDs) and polychlorinated dibenzofurans (PCDFs) are generated during the biodegradation of PCP,[30] and more harmful intermediates such as *p*-chloranil, tetrachlorohydroquinone (TeCHQ),[31] PCDDs and PCDFs[32] were produced in the treatment of PCP by AOPs. Therefore, a green and highly efficient approach for the removal of PCP is urgently necessary, by which the degradation of PCP should be significantly enhanced with the inhibition of the formation of more toxic intermediates.

As observed previously, MIP-coated TiO_2 photocatalysts not only promote the photocatalytic degradation of the target organic compounds such as 2-chlorophenol, 4-chlorophenol, 2-nitrophenol and 4-nitrophenol, but also greatly reduce the accumulation of degradation intermediates.[12,13] This suggests that we may also prepare MIP-coated TiO_2 by using PCP as the template and then use it to photocatalytically degrade PCP. However, we have found that PCP itself is not a satisfactory template from preliminary experiments. We have to find an appropriate template to prepare the MIP-coated TiO_2 for the photocatalytic removal of PCP. In the present work, on the basis of studying the interactions between the functional monomer and the template molecule under the conditions for synthesizing the MIP, we chose appropriate water-soluble structural analogues as a pseudo template and thus prepared (pseudo) molecular imprinted photocatalysts. The footprint cavities and the amino groups around the cavities are anticipated to play an important role in the photodegradation, because they may provide a special microreaction environment, which can make the benzene ring of the adsorbed PCP be better exposed to reactive OH radicals and then to be more easily cleaved for a rapid mineralization.

2. Experimental section

2.1 Materials

Degussa P25TiO_2 nanoparticles (*ca.* 80% anatase, 20% rutile; BET area, *ca.* 50 $m^2\ g^{-1}$) were used. PCP, 4-nitrophenol (4-NP), 2,4-dinitrophenol (DNP), 2,4,6-trinitrophenol (TNP) and OPDA of analytical purity, and were purchased from the Shanghai Chemical Reagent Company. Methanol (chromatographic purity) was obtained from Tedia. All these chemicals were used without further purification. Solution pH was adjusted by using diluted solutions (1 mol L^{-1}) of H_3PO_4, HCl or NaOH.

2.2 Preparation of catalyst

MIP-coated photocatalysts were prepared by coating an MIP layer on the surface of P25 nanoparticles *via in situ* polymerization of OPDA (as a functional monomer and cross-linking agent) in the presence of P25 nanoparticles and the template (the target PCP and its analogues including 4-NP, DNP and TNP). The details of the preparation procedures were similar to that described in previous work.[12,13] By varying the templates, the obtained photocatalysts were correspondingly referred to as PCP–P25, 4-NP–P25, DNP–P25 and TNP–P25. As a control, the photocatalyst NIP–P25 was synthesized when no template was used.

To verify the important role of the imprinted cavities on the MIP layer in the photodegradation, the functional amino groups on the MIP-coated TiO_2 (DNP–P25) were acetylated with acetic anhydride. Briefly, acetic anhydride (0.1 mL, 1.1 mmol) was slowly added to the catalysts (0.1 g) in dichloromethane (35 mL) in the presence of triethylamine (0.2 mL, 1.4 mmol, 1.25 equiv. of acetic anhydride). The mixture was stirred under an N_2 atmosphere for 12 h at room temperature. Excess solvent and reagents were removed by evaporation. After being washed with water and dried at room temperature, particles were obtained as amino-group-protected DNP–P25.

2.3 Characterization

The morphology of the photocatalysts was observed using high-resolution transmission electron microscopy (HRTEM) on a JEM-2010FEF TEM. FTIR spectra were recorded on a Bruker VERTEX 70 spectrophotometer, and UV-visible solid-state reflection spectra were measured on a Shimadzu UV-2550 spectrophotometer.

2.4 Photocatalytic experiments

Photocatalytic experiments were carried out in a cylindrical glass reactor, where a Philips 9 W UV lamp (λ_{max} 253.7 nm) with a quartz tube as the protective shelter was located in the axial position. After it was filled with 250 mL of an aqueous solution of PCP, the catalyst (0.1 g L^{-1}) was added, followed by an adjustment of the solution pH to 11, at which most of the PCP in solution was changed to its basic form (PCP–Na). The suspension was stirred for 20 min to favor the organic adsorption/desorption equilibrium on the catalyst surface, and the concentration of the pollutant(s) was determined as the initial concentration c_0, and then the photo-irradiation started. In order to maintain a well dispersed photocatalyst suspension, the PCP solution was homogenized with a magnetic stirrer during the UV irradiation. Aliquots (2 mL) of the solution were sampled at appropriate time intervals. The solution samples were centrifuged at 14 000 rpm (Hettich EBA21) for 15 min, and the supernatant was filtered through a 0.22 μm filter to remove the catalyst particles. The resultant solutions were used for analysis.

2.5 Analytical methods

The concentrations of the pollutants and intermediates were measured by high-performance liquid chromatography (HPLC) on a PU-2089 HPLC (JASCO), equipped with a C18 ODS column and an ultraviolet detector. The detection wavelength was set at 218 nm for PCP. In some cases, the concentrations of the pollutants and intermediates were also determined by UV-visible absorption spectrophotometry on a Cary 50 spectrophotometer (Varian). The concentrations of chloride ions and main organic acids as intermediates were monitored by ion-chromatography on a Dionex DX-500 IC

system with an ED-40 electrochemical detector operating in conductivity mode and an IonPac ICE-AS6 column. Total organic carbon (TOC) analysis was carried out by a TOC analyzer micro N/C model (Analytika jena, Germany) equipped with an automatic sample injector and a platinum based catalyst. After being extracted with *n*-heptane and esterified with acetic anhydride, major aromatic products were identified with an Agilent Technologies model 6890 gas chromatograph (GC) equipped with a 5973N mass-selective detector (He carrier gas, HP-5MS crosslinked 5% PH ME siloxane column, electron impact ionization at 70 eV). At least triplicate runs were carried out for each test, and the standard deviation was generally less than 5%.

The toxicity of the solution samples was determined by using flesh water luminescent bacterium, *Vibrio qinghaiensis* sp. *Q*67 as a detecting organism, applying the Veritas™ luminometer with a 96-well microplate (Turner BioSystems Inc., USA) according to the method reported by Zhang and coworkers.[33] The final relative light unit (RLU) measurements in various wells in the test microplate were determined after a 5 min exposure to the toxicants at 22 ± 1 °C. The toxicity of each sample was expressed as an inhibition ratio (*E*) and calculated from $E = 100\% \times (I_0 - I)/I_0$, where I_0 is an average of the RLU of *Q*67 exposed to the controls (12 parallels) and *I* is an average of the RLU to the sample (three parallels) in one microplate. At least triplicate runs were carried out for each test of the toxicity evaluation, and the standard deviation was generally less than 10%.

3. Results and discussion

3.1 Preparation of MIP-coated TiO_2 for removing PCP

3.1.1 Selection of the functional monomer. Synthesis of an MIP with molecular recognition ability requires the formation of a complex between the template and functional monomer molecules *via* chemical and/or non-chemical bonding before the polymerization. An additional requirement for the functional monomer should be considered so that the MIP layer on MIP-coated photocatalysts will not block the interactions between the photo-generated active species and the adsorbed organic pollutants, which requires the MIP to be fairly semiconducting. We have recently demonstrated that OPDA is a good function monomer,[13] because its polymerization results in polyaniline-like polymer being favorable to the separation of photo-generated electron hole pairs.[34] Therefore, OPDA is further used as the functional monomer in the present work.

3.1.2 Templates from structural analogues of PCP. As we know, the enzyme-like activity comes from the special interaction between the MIP and the template molecules. Because it was found that PCP itself is not a good template for preparing the MIP-coated photocatalyst, we checked the possible pseudo templates from the structural analogues of PCP. In order to prepare such MIP-coated photocatalysts, the structural analogues should have (i) good solubility (in water), (ii) a similar structure to the target pollutant PCP to create cavities with size and shape fitting the adsorption of the target molecules, and (iii) functional groups capable of interacting with the functional monomer. In consideration of these requirements, 4-NP, DNP and TNP were investigated as possible pseudo templates, in comparison with PCP as the real template.

The most important factor influencing the performances of the MIPs is the interaction between the functional monomer and the template molecules. Such interactions can be evaluated by comparing the UV-visible absorption spectrum of the mixture solution of the functional monomer and the template with the sum of the spectra of the individual functional monomer and template. Based on the measured spectra of the functional monomer OPDA (36.0 μmol L^{-1}), the template (36.0 μmol L^{-1}), and their mixture solution (Fig. S1, ESI†), the absorbance of the solutions at 228 nm was selected for the evaluation of the interaction between the monomer and template molecules by using the equation $F = (1 - A_{mixture}/(A_{monomer} + A_{template}))$, where *A* represents the absorbance of the compound (specified by the subscript) at 228 nm, and *F* is defined as the interaction factor hereafter, which indicates the extinction effect of the mixing due to the interaction between the monomer and template molecules. A larger *F* value means a stronger interaction between the monomer and template molecules. The values of the *F* factor in solutions at pH 2.0 were determined as 0.041, 0.130, 0.215, and 0.082 for the templates of PCP, 4-NP, DNP and TNP, respectively. Thus, the interaction between the functional monomer and template molecules increases in the template order of PCP < TNP < 4-NP < DNP. This demonstrates that the increased number of nitro groups favors the interaction between OPDA and template molecules, but the existence of three nitro groups and one –OH group in the benzene ring of TNP produces an unfavorable effect of steric hindrance. After the interaction between the functional monomer and the template molecules was clarified, a series of MIP-coated photocatalysts were prepared by using PCP, 4-NP, DNP or TNP as templates, and the resultant MIP-coated photocatalysts were referred to as PCP–P25, 4-NP–P25, DNP–P25 and TNP–P25, correspondingly. A control photocatalyst NIP–P25 was similarly obtained but in the absence of any template.

3.1.3 Optimization of pH and feed ratio of monomer to template. The effects of solution pH on the *F* factor between DNP and OPDA were studied (Fig. S2, ESI†), and the influences of the molar ratio of OPDA to DNP on the catalytic activity compared to DNP–P25 were investigated (Fig. S3, ESI†). Based on these experimental results, two important synthetic parameters were optimized at pH 2.0 and the molar ratio of OPDA to DNP at 4 : 1.

3.2 Characterization of MIP-coated photocatalysts

The morphology of the MIP-coated photocatalysts was observed with HRTEM, which indicated that the TiO_2 core in DNP–P25 was partially coated with a layer of MIP, having a thickness of ~5 nm (Fig. S4, ESI†). Furthermore, the MIP coating on the surface of TiO_2 particles was shown by the UV-vis solid-state reflection spectra of neat P25 and DNP–P25 particles. In comparison with the neat P25, DNP–P25 prolongs the absorption in the visible region (Fig. S5, ESI†). Main characteristic peaks of poly-*o*-phenylenediamine (POPD) and

TiO_2 were observed in the FTIR spectra of the imprinted photocatalysts (Fig. S6, ESI†). However, in comparison to the main bands of pure POPD at 1523 cm^{-1} (the bending mode of the N–H bond), 1229 and 1346 cm^{-1} (=C–N stretching on the benzene ring), all the bands were shifted to higher wavenumbers when the polymer layer was coated on TiO_2. Furthermore, a sharp peak at 1619 cm^{-1} being associated with the C=N stretching vibration was shifted to 1627 cm^{-1} with increasing MIP layer thickness. These results indicate the novel structure of the imprinted photocatalysts may cause the interface interaction between the MIP layer and TiO_2 core, and the chemical bond interaction is useful to transfer charge carriers and induce the enhancing effect on the photocatalytic activity.

3.3 Enhanced catalytic ability of DNP–P25 photocatalyst

Fig. 1 shows the kinetics of direct photolysis and photocatalytic degradation of PCP over different photocatalysts, which indicates that all the degradation processes follow a pseudo first-order reaction. It is clearly seen from Fig. 1 that the direct photolysis of PCP is the slowest. The added TiO_2 will adsorb UV light, resulting in the decreasing of the direct photolysis. Thus, the photocatalytic process is the dominant one in the photodegradation of PCP over DNP–P25. This was confirmed by the much enhanced degradation of PCP over DNP–P25. The apparent rate constant (k) for PCP degradation has an order of DNP–P25 > 4-NP–P25 > TNP–P25 > P25 > PCP–P25 > NIP–P25 > direct photolysis. The enhancing or depressing effect can be compared by the value of $k_{photocatalyst}/k_{P25}$, which was determined as 0.62, 0.79, 1.31, 1.49 and 2.75 for NIP–P25, PCP–P25, TNP–P25, 4-NP–P25 and DNP–P25, respectively. These results confirm that DNP is the best template.

Because $k_{PCP-P25}/k_{P25} = 0.79 < 1$, PCP is not an appropriate template for preparing MIP-coated photocatalysts to remove the target pollutant PCP. This is possibly due to either the poor interaction between the functional monomer and PCP molecules, or a very limited solubility of PCP in the solution of synthesis. The above experimental results demonstrate that some organic compounds cannot be used as the templates for preparing the MIP-coated photocatalysts to remove them as pollutants in the environment, but it is possible to find an appropriate structural analogue of the target pollutant for preparing the required MIP-coated photocatalyst.

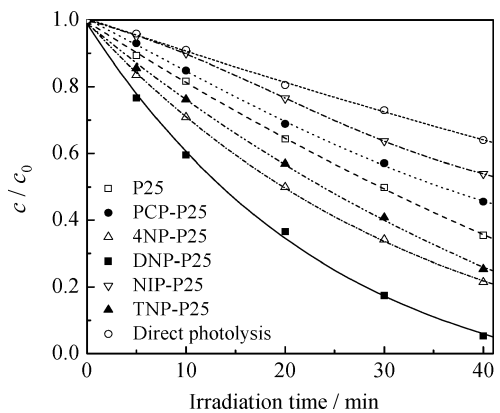

Fig. 1 Kinetics of direct photolysis and photocatalytic degradation of PCP (c_0 30 mg L^{-1}, pH 11) over different photocatalysts. The rate constant of the direct photolysis is 0.0112 min^{-1}, and that over P25, PCP–P25, NIP–P25, 4-NP–P25, DNP–P25 and TNP–P25 is 0.0254, 0.0198, 0.0158, 0.0378, 0.0699 and 0.0332 min^{-1}, respectively.

3.4 Inhibited generation of harmful intermediates

It is feared that the photocatalytic oxidation of PCP on TiO_2 could produce more harmful intermediates and by-products. Mills and Hoffmann[35] reported that the photooxidation of PCP over TiO_2 proceeds *via* the attacking of a hydroxyl radical at the *para* position on the benzene ring to form a semiquinone radical which in turn disproportionates to yield *p*-chloranil and TCHQ, being possibly followed by a further degradation. The toxic dimeric intermediates such as PCDDs and PCDFs were also found by other groups.[36,37] It is necessary to clarify if these more toxic intermediates are inhibited or not when PCP is degraded over DNP–P25, which was performed by UV-visible absorption and GC/MS measurements.

Firstly, the UV-visible absorption spectra of the PCP solution (5 mg L^{-1}, pH 11) were monitored during the degradation as shown in Fig. 2. In the case of P25, two new absorption peaks were observed at about 280 nm and 310 nm, being consistent with the report that the intermediates TCHQ and *p*-chloranil had absorptions at 308 nm and 284 nm, respectively,[36] and another new absorption band in the region from 320 nm to 410 nm was similar to the absorptions of the dibenzodioxins/furans.[22] However, the PCP photodegradation over DNP–P25 was much faster than over P25, and the accumulation of the aromatic intermediates over DNP–P25 was almost unobservable (as seen in the region from 240 to 325 nm). This indicates that DNP–P25 not only promotes the photodegradation of the parent pollutant, but also inhibits the generation of the highly toxic intermediates, being favorable to the complete mineralization of PCP.

Secondly, the reaction products were identified with GC/MS by using 1,2-dibutylphthalate (DBP) as the internal standard after the solution was esterified with acetic anhydride and then extracted with heptane. The GC/MS chromatograms for the PCP solutions irradiated over P25 and DNP–P25 for 21 min are shown in Fig. 3. Besides dichlorophenol (DCP), many aromatic intermediates and by-products are found after the degradation of PCP over P25, which include TeCHQ, tetrachlorocatechol (TeCC), acetoxypentachlorophenyl (APCP), tetrachlorodibenzo-*p*-dioxin (TeCDD), pentachlorodibenzo-*p*-dioxin (PCDD), hexachlorodibenzo-*p*-dioxin (HexCDD), heptachlorodibenzo-*p*-dioxin (HepCDD) and octachlorodibenzo-*p*-dioxin (OCDD). These intermediates are more stable and harmful than PCP to human beings.[37] Thus, the PCP photodegradation on P25 may increase the toxicity of the solution, which must be forbidden from the view point of environmental protection. Excitingly, the toxic aromatic intermediates are almost inhibited in the case of DNP–P25. Therefore, the photodegradation by using DNP–P25 is a safe and green approach of removing PCP.

Thirdly, the accumulation of Cl^- ions and main organic acids was also monitored during the photodegradation of PCP by using ion-chromatography. Fig. 4 shows the profile of

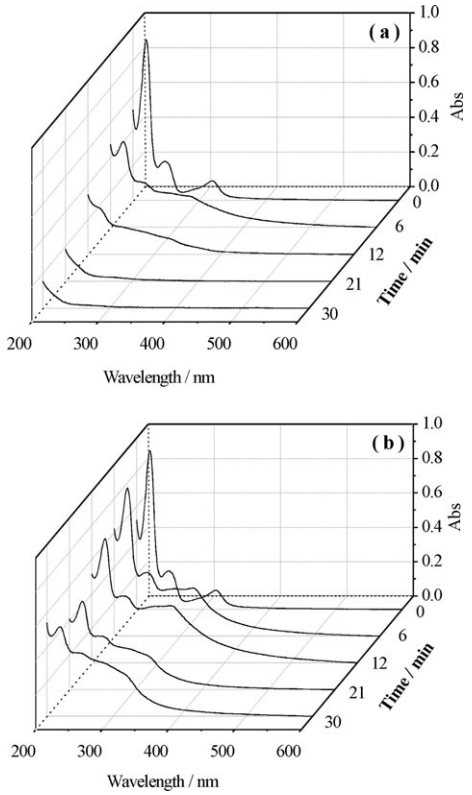

Fig. 2 UV-visible absorption spectra of the PCP solution (5 mg L^{-1}, pH 11) recorded during the photodegradation over DNP–P25 (a) and P25 (b).

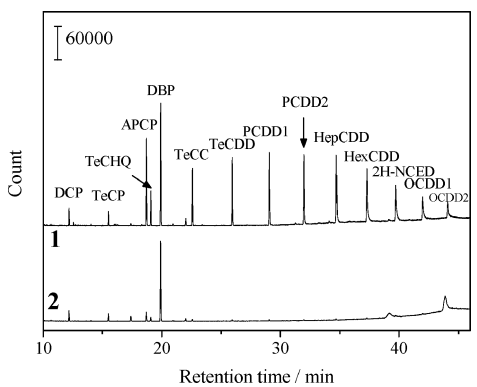

Fig. 3 GC/MS chromatograms of the heptane extract of the reaction mixtures degraded over P25 (1) and DNP–P25 (2) at pH 11 for 21 min of irradiation. Esterification of the solution was performed with acetic anhydride before the heptane extraction.

Cl^- ions in the PCP solutions during the degradation, where Cl^- ions were generated from the dechlorination of PCP. The releasing of Cl^- ions is rapid in the initial stage and slow in the later stage on P25, being similar to the observation of Mills and Hoffmann.[35] In comparison with P25, DNP–P25 yields much faster dechlorination of PCP, and gives an almost complete dechlorination of PCP after 50 min of illumination. This further confirms that DNP–P25 can accelerate the degradation and dechlorination of PCP.

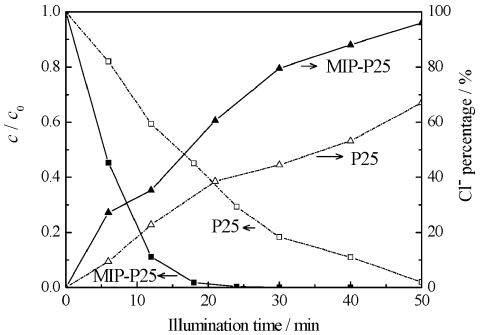

Fig. 4 Effects of illumination time on the degradation and dechlorination of PCP (c_0 5 mg L^{-1}) over P25 and MIP–P25 (i.e. DNP–P25).

Table 1 gives the distribution of the intermediates during the PCP photodegradation. Here, the intermediates include total inorganic carbon (TIC), organic acids, and aromatic intermediates. The generated organic acids (such as formic, acetic, and dichloromaleic acids) were determined by ionic chromatography (Fig. S7, †), and the TOC of the solution was also measured. TIC was simply obtained by subtracting the initially added TOC from the measured TOC after the degradation, and the amount of the newly generated aromatic intermediates was obtained by subtracting the measured TOC from the measured amount of simple organic acids detected. It is seen from Table 1 that after an illumination of 21 min, DNP–P25 converted 95.67% of the carbon in the initial PCP solution into inorganic carbon (39.65%) and small organic acids (52.58%) with a small production of aromatic intermediates (3.44%, including DCP and TCP), whereas the neat P25 converted only 75.31% of PCP into inorganic carbon (18.07%) and small organic acids (29.03%) with a large production of aromatic intermediates (28.21%). The much depressed generation of more toxic aromatic intermediates by using DNP–P25 is consistent with the above-discussed GC/MS analysis. This strongly demonstrates that the ring of PCP is cleaved much more rapidly and completely during the degradation over DNP–P25 than over P25.

As discussed above, a fairly large amount of more toxic and stable aromatic intermediates are generated during the photodegradation of PCP over P25, indicating that the photocatalytic degradation is not a safe approach for removing PCP. By using DNP–P25, the PCP degradation is drastically accelerated and the generation of aromatic intermediates is significantly inhibited. Hence, the photocatalytic degradation can become a safe approach of removing PCP by using DNP–P25. To confirm it, the toxicity of the PCP solution during its photodegradation on P25 and DNP–P25 was monitored by using the luminescent bacterium *Q*67, and the inhibition ratio (*E*) can represent the toxicity of the solution. As shown in Fig. 5, the toxicity of the solution decreased slightly during the degradation of PCP over P25, which reflects a combination of the toxicity-decreasing effect from the removal of PCP and the toxicity-increasing effect from the generation of aromatic intermediates. However, the PCP solution was rapidly detoxified by DNP–P25, which is attributed to the accelerated removal of PCP and the inhibited formation of more harmful aromatic intermediates.

Table 1 Carbon mass balance (%) in the 5 mg L^{-1} PCP solution system after irradiation of 6 min and 21 min over P25 and DNP–P25

State of carbon	Over P25		Over DNP–P25	
	After 6 min	After 21 min	After 6 min	After 21 min
TIC	7.55	18.07	8.06	39.65
Formic acid	1.12	1.55	1.33	2.21
Acetic acid	13.54	13.72	33.34	21.82
Oxalic acid	2.43	6.20	3.76	7.95
Dichloromaleic acid	3.12	7.56	15.08	19.86
Residual PCP	68.87	24.69	38.25	4.33
Total of detected carbon	95.07	71.79	99.82	96.56
New aromatic toxicant	**4.93**	**28.21**	**0.08**	**3.44**

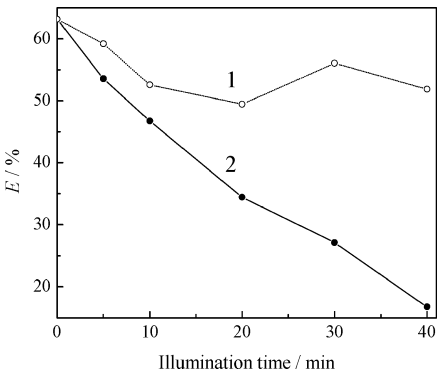

Fig. 5 Variation of the inhibition ratio (E) of the PCP (c_0 30 mg L^{-1}, pH 11) solution to $Q67$ during its photocatalytic degradation over P25 (1) and DNP–P25 (2).

3.5 Tentative explanation of the enhanced degradation of PCP over DNP–P25

In the suspension of DNP–P25, the interaction between the target (PCP) and the MIP substrate results in the formation of a moderately stable complex (PCP–MIP) between the target and MIP. Under the photocatalytic action of TiO_2, the PCP–MIP complex is oxidized, leading to the degradation of PCP and the recovery of MIP. This is similar to the process of enzyme catalysis. In order to explain the enhanced degradation of PCP over DNP–P25, the photocatalytic degradation of PCP at concentrations ranging from 2 to 50 mg L^{-1} was conducted over DNP–P25, and the initial rate (v, in the time window from 0 to 20 min) for the degradation of PCP was obtained. As a control, 5 or 10 mg L^{-1} of the used template DNP was added as an inhibitor to the solutions of PCP, and the initial rate of PCP degradation was obtained similarly. The experimental data were fitted with Lineweaver–Burk double reciprocal plots ($v^{-1} \sim c_0{}^{-1}$), as shown in Fig. 6. It is found from Fig. 6 that the slopes of the reciprocal plots of the rate *vs.* substrate concentration exhibit the characteristics of noncompetitive inhibition.[38,39] The inhibition constants were calculated from eqn (1),

$$\frac{1}{\nu} = \frac{K_m}{\nu_{max}}\left(1 + \frac{[I]}{K_i}\right)\frac{1}{[c]} + \frac{1}{\nu_{max}}\left(1 + \frac{[I]}{K_i}\right) \qquad (1)$$

where v is the initial reaction rate of PCP degradation, ν_{max} is the maximal rate of PCP degradation, $[c]$ is the concentration of PCP, $[I]$ is the inhibitor concentration, K_m is the Michaelis–Menten constant, and K_i represents the dissociation constants for the enzyme–inhibitor (EI) complex.

Accordingly, when the concentration of DNP was increased from 0 to 10 mg L^{-1}, a significant decrease of ν_{max} was found from 1.74 min^{-1} to 0.79 min^{-1}. However, the addition of DNP did not affect K_m, which confirms that DNP is working through a traditional reversible and noncompetitive (non-repulsive) mechanism of inhibition. This is very important; because DNP–P25 is prepared by using DNP as the template, it is reasonable that DNP–P25 can distinguish DNP from PCP molecules in the solution by the recognition ability of the MIP layer. If the molecular recognition ability is perfect, DNP–P25 cannot be used to degrade PCP. It is fortunate that the footprint cavities in the MIP layer on the surface of DNP–P25 can be shared by both DNP and PCP for their adsorption and then degradation. This indicates that PCP molecules are able to be adsorbed on DNP–P25 almost as easily as the used template DNP, which is confirmed further by the evaluated affinity of PCP and DNP over DNP–P25.

To clearly demonstrate the affinity of PCP and DNP over DNP–P25, eqn (1) can be simply changed to eqn (2), being named as the Dixon equation.[40]

$$\frac{1}{\nu} = \frac{1}{\nu_{max}K_i}\left(1 + \frac{K_m}{[c]}\right)[I] + \frac{1}{\nu_{max}}\left(1 + \frac{K_m}{[c]}\right) \qquad (2)$$

K_i for the photocatalysis can be calculated by using eqn (2). Under the experimental conditions, the K_i value of the used template (DNP) over DNP–P25 was obtained as 8.85, whereas the K_m value of the substrate (PCP) was evaluated as 19.88. Thus, the affinity ($1/K_m$) of PCP on DNP–P25 is only slightly

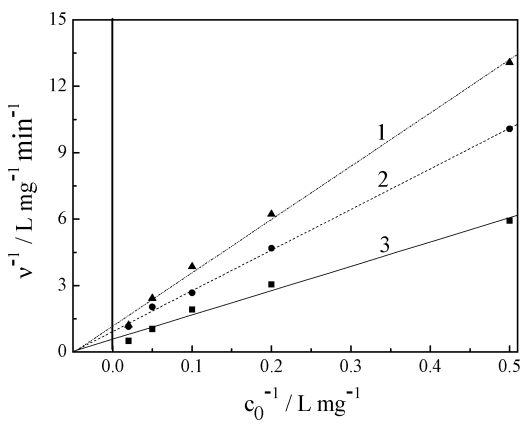

Fig. 6 Lineweaver–Burk double reciprocal plots for the photocatalytic degradation of PCP at different concentrations in the presence of DNP (as an inhibitor) at concentrations of (1) 10, (2) 5 and (3) 0 mg L^{-1}.

weaker than that ($1/K_i$) of DNP on DNP–P25. This high affinity leads to the enhanced photodegradation of PCP on DNP–P25.

Like previously reported MIP-coated TiO_2 photocatalysts, DNP–P25 promoted the photocatalytic degradation of the template molecules of DNP and reduced the accumulation of degradation intermediates, but the types of the intermediates generated in the DNP degradation on DNP–P25 were almost the same as that on neat P25 (Fig. S8 and S9, ESI†). This is very different from the degradation of PCP on DNP–P25, because the numbers of the degradation intermediates produced on DNP–P25 are much lower than that on neat P25 (Fig. 3). This suggests that the mechanism of the PCP degradation on DNP–P25 is different from that on neat P25. The unusual behavior for the degradation of PCP over DNP–P25 should be related to the interaction between PCP molecules and the amino groups fixed in the footprint cavities of the MIP layer. To understand it, the functional amino groups in the footprint cavities were acetylated *via* acetic anhydride, and the acetylated DNP–P25 was used to photocatalytically degrade PCP (5 mg L^{-1}). It was found that the degradation rate of PCP over the acetylated DNP–P25 was considerably slower than that over DNP–P25 without the acetylation. This indicates that the amino groups in the footprint cavities are very important to binding PCP molecules. Moreover, by observing the absorption of the solution from 235 nm to 435 nm during the photocatalytic degradation of PCP, which mainly consisted of the toxic compounds in the solution (such as remaining PCP and the generated aromatic intermediates), it was found that the amounts of the toxic compounds in the solution had an increasing order on the photocatalysts of DNP–P25 < TNP–P25, 4-NP–P25, < NIP–P25 < P25. This indicates that the functional groups around the cavities of the MIP greatly affect the inhibition of the generation of the toxicants, and only the cavities tailored with DNP as the template are appropriate.

Based on above discussion, mechanisms of the photocatalytic degradation of PCP over the different catalysts are proposed in Scheme 1. In the case of neat P25 TiO_2, PCP molecules are simply adsorbed on the surface of P25, and chemical attack is allowed from almost all directions, leading to easy generation of complicated degradation intermediates (Scheme 1a). The rather loosely adsorbed degradation intermediate may diffuse into the solution before its further degradation, and then convert into more harmful by-products as in the report of Kim and coworkers.[36] Similar situations will occur when NIP–P25 is used instead of neat P25. When 4-NP is used as pseudo template, the footprint cavities of 4-NP–P25 are considered to be formed with three amino groups (Scheme 1b). Once the PCP molecules are rebound to the adsorption sites at these imprinted cavities, only the –OH and two –Cl could bind with the MIP, the other directions of PCP are free and can be attacked by the photo-generated oxidizing species such as OH radicals. As the oxidizing species can attack the ring of PCP bilaterally, the degradation of PCP over 4-NP–P25 may be similar to that over neat P25 TiO_2. When TNP is applied as the template, the footprint cavities of TNP–P25 are composed of seven amino groups (Scheme 1c), making the size of the cavities much larger than the size of the

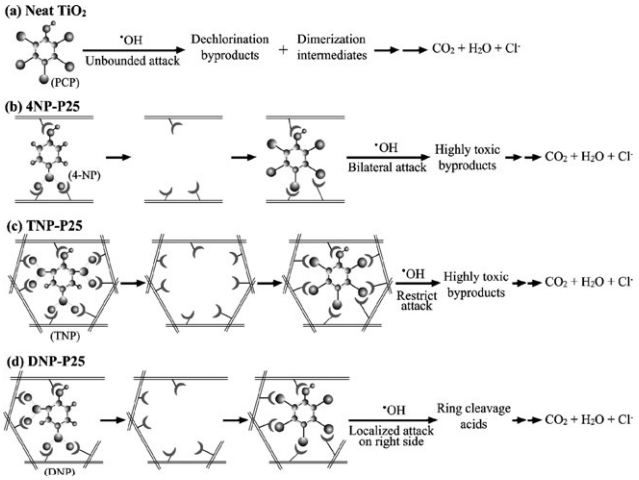

Scheme 1 Mechanisms of the photodegradation of PCP over different photocatalysts.

PCP molecules. This cannot tightly fix the PCP molecules in the cavities, resulting in the generation of various intermediates like in the cases of P25 and 4-NP–P25.

However, in the case of DNP–P25, the PCP molecules can be adsorbed over the imprinted cavities on the MIP layer *via* the formation of a moderately stable complex (PCP–MIP) between PCP and MIP. In this way, the PCP molecules are fixed into a well-defined micro environment (Scheme 1d). As the hydrogen-bonding interaction between DNP and MIP is dissymmetric, the electron atmosphere of PCP is thus sloped to the left side, meaning that the ring of PCP is easy to open. On the other hand, only one Cl atom of the adsorbed PCP molecule is not protected by amino groups; the oxidizing species will attack the molecule *via* this Cl atom, making the C–Cl and C–C bonds be cleaved more easily here. The enhanced splitting of the benzene ring inhibits the formation of more harmful aromatics, due to its preventing the dimerization and/or coupling of the initial intermediates from the degradation of PCP. In this way, DNP–P25 can select a green and safe pathway to remove PCP.

4. Conclusion

The photocatalytic degradation of PCP over neat TiO_2 not only was slow, but also produced various highly toxic intermediates. To achieve a fast and safe removal of PCP from aqueous solutions with complete inhibition of the generation of the toxic intermediates, DNP–P25 was synthesized as a MIP-coated photocatalyst by using molecular imprinting technique with DNP as a pseudo template. Relative to naked P25 TiO_2, the pseudo MIP-coated photocatalyst DNP–P25 significantly promoted the dechlorination and degradation of PCP due to its enzyme-like catalytic effects. Due to the similar chemical structures of PCP and DNP, the affinity of PCP over the photocatalyst DNP–P25 was comparable with that of the used template DNP. More interestingly, the generation of highly toxic intermediates was greatly depressed during the photocatalytic degradation of PCP over DNP–P25. The unique behavior of PCP degradation over DNP–P25 was related to the special interactions between the adsorbed PCP

molecules and the amino groups at the footprint cavities of the MIP layer. From the view point of removing highly-toxic low-level organic pollutants using a photocatalytic degradation technique, the findings in the present work are very suggestive because it is possible to prepare a MIP-coated TiO_2 photocatalyst by using an appropriate structural analogue of the target pollutant as the template, and then use it to photocatalytically degrade the target pollutant without the generation of highly toxic intermediates, being confirmed as a green and safe approach.

Acknowledgements

This research was supported by the National Natural Science Foundation of China (Grant Nos. 20677019 and 20877031) and the State Key Laboratory of Pollution Control and Resource Reuse Foundation (No. PCRRF08007). The Analytical and Testing Center of Huazhong University of Science and Technology is thanked for its help in the characterization of the catalysts.

References

1 A. Leonhardt and K. Mosbach, *React. Polym., Ion Exch., Sorbents*, 1987, **6**, 285.
2 K. M. Shokat, C. J. Leumann, R. Sugasawara and P. G. Schultz, *Nature*, 1989, **338**, 269.
3 R. Weinstain, R. A. Lerner, C. F. Barbas, III and D. Shabat, *J. Am. Chem. Soc.*, 2005, **127**, 13104.
4 K. Polborn and K. Severin, *Chem. Eng. J.*, 2000, **6**, 4604.
5 A. Jakubiak, B. N. Kolarz and J. Jezierska, *Macromol. Symp.*, 2006, **235**, 127.
6 M. Emgenbroich and G. Wulff, *Chem.–Eur. J.*, 2003, **9**, 4106.
7 D. Lavabre, J. Micheau, J. R. Islas and T. Buhse, *J. Phys. Chem. A*, 2007, **111**, 281.
8 O. Ramström and K. Mosbach, *Curr. Opin. Chem. Biol.*, 1999, **3**, 759.
9 G. Wulff, *Chem. Rev.*, 2002, **102**, 1.
10 Y. Paz, *C. R. Chim.*, 2006, **9**, 774.
11 M. Fukushima and K. Tatsumi, *Environ. Sci. Technol.*, 2005, **39**, 9337.
12 X. Shen, L. Zhu, J. Li and H. Tang, *Chem. Commun.*, 2007, 1163.
13 X. Shen, L. Zhu, G. Liu, H. Yu and H. Tang, *Environ. Sci. Technol.*, 2008, **42**, 1687.
14 X. Shen, L. Zhu, H. Yu, H. Tang, S. Liu and W. Li, *New J. Chem.*, 2009, **33**, 1673.
15 X. Shen, L. Zhu, C. Huang, H. Tang, Z. Yu and F. Deng, *J. Mater. Chem.*, 2009, **19**, 4843.
16 J. P. Wilcoxon, *J. Phys. Chem. B*, 2000, **104**, 7334.
17 K. Hoshino, R. Watanabe and M. Takano, *J. Biotechnol.*, 2008, **136**, S704.
18 D. Boyle, *J. Environ. Manage.*, 2006, **80**, 380.
19 S. Singh, R. Chandra, D. K. Patel, M. M. K. Reddy and V. Rai, *Bioresour. Technol.*, 2008, **99**, 5703.
20 E. L. Puplampu and D. K. Dodoo, *J. Photochem. Photobiol., A*, 2000, **135**, 81.
21 J. Hong, D. Kim, C. Cheong, S. Jung, M. Yoo, K. Kim, T. Kim and Y. Park, *Anal. Sci.*, 2000, **16**, 621.
22 S. Vollmuth, A. Zajc and R. Niessner, *Environ. Sci. Technol.*, 1994, **28**, 1145.
23 J. Xue and J. Wang, *J. Environ. Sci.*, 2008, **20**, 1153.
24 M. Sung, S. Z. Lee and C. P. Huang, *J. Contam. Hydrol.*, 2008, **98**, 75.
25 L. K. Weavers, N. Malmstadt and M. R. Hoffmann, *Environ. Sci. Technol.*, 2000, **34**, 1280.
26 M. A. Oturan, N. Oturan, C. Lahitte and S. Trevin, *J. Electroanal. Chem.*, 2001, **507**, 96.
27 Z. Gao, S. Yang, C. Sun and J. Hong, *Sep. Purif. Technol.*, 2007, **58**, 24.
28 Y. Guo, X. Quan, N. Lu, H. Zhao and S. Chen, *Environ. Sci. Technol.*, 2007, **41**, 4422.
29 J. Gunlazuardi and W. A. Lindu, *J. Photochem. Photobiol., A*, 2005, **173**, 51.
30 L. G. Öberg and C. Rappe, *Chemosphere*, 1992, **25**, 49.
31 W. F. Jardim, S. G. Moraes and M. M. K. Takiyama, *Water Res.*, 1997, **31**, 1728.
32 W. Liu, X. Quan, Q. Cui, M. Ma, S. Chen and Z. Wang, *Ecotoxicol. Environ. Saf.*, 2008, **71**, 267.
33 Y. Zhang, S. Liu, X. Song and H. Ge, *Ecotoxicol. Environ. Saf.*, 2008, **71**, 880.
34 J. Li, L. Zhu, Y. Wu, H. Yutaka, A. Zhang and H. Tang, *Polymer*, 2006, **47**, 7361.
35 G. Mills and M. R. Hoffmann, *Environ. Sci. Technol.*, 1993, **27**, 1681.
36 J. Kim, K. Choi, I. Cho, H. Son and K. Zoh, *J. Hazard. Mater.*, 2007, **148**, 281.
37 A. Hirvonen, M. Trapido, J. Hentunen and J. Tarhanen, *Chemosphere*, 2000, **41**, 1211.
38 L. Casella, M. Gullotti, E. Monzani, L. Santagostini, G. Zoppellaro and T. Sakurai, *J. Inorg. Biochem.*, 2006, **100**, 2127.
39 M. C. Pirrung, H. Liu and A. T. Morehead, Jr., *J. Am. Chem. Soc.*, 2002, **124**, 1014.
40 M. Dixon and E. C. Webb, *Enzymes*, Academic Press, New York, 1979.